Electric ionization lasers

N. G. Basov, É. M. Belenov, V. A. Danilychev, O. M. Kerimov, I. B. Kovsh, A. S. Podsosonnyĭ, and A. F. Suchkov

P. N. Lebedev Physics Institute of the Academy of Sciences USSR

A description is given of the electric ionization method for the excitation of active media in gas lasers. A dense gas is made conducting by ionizing radiation provided by an external source. If a current is passed through the gas, the energy provided by the external source can be converted into the excitation energy of active levels of molecules. The mechanism of the introduction of energy into the active medium of an electric ionization gas laser is discussed and the excitation of active laser levels is considered. The experimental results are given of an investigation of a CO_2 electric ionization laser filled with a mixture of CO_2, N_2, and He and operating at total pressures up to 50 atm. A specific output power of $\sim 10^6 \, W/cm^3$ in the form of pulses of $\sim 10^{-7}$ sec duration is reported. The current, threshold, and energy characteristics are given. The dependences of the gain on the pressure and composition of the mixture are reported and the emission spectrum of the laser is described. The possibility of continuous frequency tuning and of generation of high-power ultrashort pulses is considered.

In 1964 Patel achieved laser emission with the aid of rotation-vibrational transitions in gaseous carbon dioxide and reported that the efficiency of a laser of this type could reach several tens of percent.[1] In the last two years Dumanchin and Rocca-Serra, working at the CGE laboratories at Marcoussis in France,[2] Beaulieu in Canada,[3] and Wood et al. in the USA[4] employed transverse discharges and reached megawatt power levels and high efficiencies in pulsed CO_2 lasers. High output powers in units of a very moderate size were obtained by increasing the pressure of the active gas from tenths of an atmosphere, as used in a conventional gas-discharge laser, to 1 atm.

The present paper describes a new type of gas laser, which is the electric ionization laser operating at high pressures up to tens of atmospheres. This laser was built early in 1971.[5] Similar lasers were recently commissioned in the USA and in Australia.[6,7] The electric ionization laser is based on theoretical and experimental investigations of electron-beam excitation.[8] These investigations have demonstrated that the excitation of molecular gas lasers with fast electrons and other high-energy particles suffers from a very low efficiency. High-energy particles can be used effectively only in the excitation of condensed gases and solids. However, it has been found that the output power of gas-discharge lasers can be increased somewhat by irradiation with high-energy particles.[9,10] In this case, the action of high-energy particles on the gas discharge does not alter basically the excitation mechanism. In particular, an increase in the pressure of the active mixture above 30 Torr stops the laser action.[10]

The basis of the method discussed in the present paper is the establishment of conductivity in a dense gaseous medium by ionization radiation provided by an external source. If an electric current is passed through the gas, practically all the energy of this current can be transformed into the vibrational energy of molecules. It must be stressed that in a gas-discharge laser the discharge electrons perform a dual role: they participate in the conduction process and induce the conductivity by direct ionization. In the laser described here, these two functions are separated and this makes it possible to avoid several important disadvantages of the gas-discharge excitation method. In particular, it is possible to reach very high efficiencies and to achieve

uniform excitation of a compressed gas without filamentation.

Eletskiĭ and Smirnov[11] considered the possibility of excitation of a CO_2 laser via photoionization of cesium vapor; they adopted the charge transfer model first put forward by Thomson.[12] The electric current in such a system is governed by the mobility of the ionic component because of the spatial separation of the charge and the value of this current is very small even when the degree of ionization of the gas is high. According to this model, it would be practically impossible to build an electric ionization laser.

Experimental investigations[13,14] demonstrated that large currents could flow in ionized gases provided the degree of ionization was sufficiently high.[15] The electron density should be higher than a certain value governed by the nature of the gas, the pressure, and the distance between the electrodes. It is found[15] that in a highly ionized gas the electric field in the electron-depleted cathode layer reaches a value considerably higher than the ionization threshold of the gas. The density of electron pairs increases because of the Townsend multiplication and the ionic conductivity in the cathode layer reaches a value equal to the electronic conductivity in the rest of the system. This is possible because, on the whole, the concentration of neutral atoms in a gas is many orders of magnitude higher than the electron density. Thus, the cathode layer of the gas acts as an inexhaustible electron emitter. The emission rate is maintained automatically at the level set by the conductivity of the rest of the system. The cathode layer is found to be very thin.

We shall now consider the mechanism of the flow of a current in the active medium of an electric ionization laser and the mechanism of excitation of active levels. We shall then give the results of an experimental investigation of a CO_2 electric ionization laser.

THEORY

1. Mechanism of introduction of energy into the active medium of an electric ionization gas laser

The processes accompanying the transfer of charge in the active medium of an electric ionization laser can be described by the following system of equations:

$$\frac{\partial n_e}{\partial t} + \operatorname{div} n_e v_e = \alpha v_e n_e + \left(\frac{\partial n}{\partial t}\right)_i - b n_e n_i - c N_0 n_e,$$

$$\frac{\partial n_i}{\partial t} + \operatorname{div} n_i v_i = \alpha v_e n_e + \left(\frac{\partial n}{\partial t}\right)_i - b n_e n_i,$$

$$\frac{\partial E}{\partial x} = 4\pi e (n_i - n_e), \tag{1}$$

$$\int_0^L E(x)\,dx = U, \quad \int_0^L (n_i - n_e)\,dx = 0,$$

$$[j_e + \beta j_i + j_a]_{x=0} = [j_e]_{x=L},$$

where n_e and n_i are, respectively, the electron and ion densities; v_e and v_i are the drift velocities of electrons and ions; $\alpha(E)$ is the first Townsend coefficient describing the process of avalanche multiplication of electrons in a high-field region; $(\partial n/\partial t)_i$ is the rate of supply of electrons by the external ionization source; b and c are the recombination and trapping coefficients; N_0 is the concentration of molecules; j_e and j_i are, respectively, the electronic and ionic components of the current; j_f is the field-emission current; β is the coefficient of secondary electron emission resulting from the bombardment of the cathode with ions.

The system (1) can be integrated approximately. It is found that in fields U/L below the static breakdown value the avalanche ionization process is effective only in a narrow region near the cathode and the thickness of this region is Δx. Outside this region $(x > \Delta x)$ the steady-state electron density $n_e = N_e$ is independent of x and is given by the relationship

$$(\partial n/\partial t)_i = b N_e^2 + c N_0 N_e. \tag{2}$$

If

$$p \approx 10^4 \text{ Torr}, \quad U/pL = 10 \text{ V/cm} \cdot \text{Torr}, \quad N_e \approx 10^{14} \text{ cm}^{-3} \tag{3}$$

the cathode potential drop $\varphi = E(0)\Delta x$ amounts to 10^3 V and the width of the cathode region is $\Delta x \approx (1-2) \times 10^{-4}$ cm. Thus, the external field is not screened and the current is governed by the usual Ohm's law for a medium whose conductivity is induced by an external ionization source. If the parameters are given by Eq. (3) and the duration of the ionization pulse is 2×10^{-8} sec, the energy which can be introduced into the active medium is $\sim 0.3{-}0.4$ J/cm^3.

By way of example, we shall consider the cathode layer in pure nitrogen. In the range $40 \text{ V} \cdot \text{cm}^{-1} \cdot \text{Torr}^{-1} \le E/p \le 200 \text{ V} \cdot \text{cm}^{-1} \cdot \text{Torr}^{-1}$ the Townsend coefficient of nitrogen can be represented in the form[16]

$$\alpha = pA(E/p - B)^2, \tag{4}$$

where $A = 1.17 \times 10^{-4}$ cm $\cdot$ Torr $\cdot$ V^{-2}, $B = 32.2$ V $\cdot$ cm^{-1} Torr^{-1}. It follows from[16] that in the 40 V $\cdot$ cm$^{-1} \cdot$ Torr$^{-1} \le E/p \le 200$ V $\cdot$ cm$^{-1} \cdot$ Torr^{-1} range the drift velocity of ions varies weakly with E/p, and, therefore, we can assume that v_i is constant. We shall also postulate[17] that the field in the cathode region decreases linearly. This assumption of the linear distribution of the field intensity in the cathode layer is supported quite strongly by the experimental results.[17]

Subject to the assumptions made above, the system (1) yields the following expressions for the parameters of the cathode layer:

$$\varphi = \left[C \left(\frac{N_e E/p}{p^2} \right)^{1/2} + B \right]^2 \frac{Dp^2}{N_e E/p} \tag{5}$$

$$\frac{E(0)}{p} = C \left(\frac{N_e E/p}{p^2} \right)^{1/2} + B, \tag{6}$$

$$d = 2\varphi / E(0). \tag{7}$$

Here, φ is the cathode drop of the potential, $E(0)$ is the field intensity on the surface of the cathode, d is the thickness of the cathode layer, and N_e is the steady-state electron density far from the cathode region. The constants C and D are given by

$$C = \left(\frac{12\pi\mu_e \cdot 1.44 \cdot 10^{-7}}{A v_i} \ln \frac{1}{\beta} \right)^{1/2}, \tag{8}$$

$$D = v_i / 8\pi\mu_e \cdot 1.44 \cdot 10^{-7}, \tag{9}$$

where μ_e is the electron mobility in cm$^2 \cdot$ Torr $\cdot$ sec^{-1} and v_i is measured in cm/sec.

We shall consider a numerical example of nitrogen with $N_e = 2 \times 10^{12}$ cm^{-3} at a pressure $p = 10^4$ Torr. Following,[17] we shall assume that $\mu_e = 4.5 \times 10^5$ cm$^2 \cdot$ Torr $\cdot$ sec^{-1} and $v_i = 9 \times 10^4$ cm/sec. The results of calculations for a range of values of E/p are given below:

E/p, V $\cdot$ cm^{-1} $\cdot$ Torr^{-1}:	5	10	15	20
E(0)/p, V $\cdot$ cm^{-1} $\cdot$ Torr^{-1}:	79	92	101	107
d, 10^{-3} cm:	8,8	5,1	3,9	3
φ, V:	3500	2330	1870	1610

These results were obtained for a distance of 1 cm between the electrodes. It follows from the results that the cathode drop of the potential does not exceed more than several percent of the total applied voltage. If the electron density N_e is increased, it follows from Eq. (5) that the thickness d decreases with decreasing cathode drop, and the field near the cathode increases.

We shall now give the results of calculations of the parameters of the cathode layer for $N_e = 5 \times 10^{14}$ cm^{-3} and $p = 10^4$ Torr. In these calculations we used different approximations for the dependences of α/p and v_i on E/p in the 200 V $\cdot$ cm$^{-1} \cdot$ Torr$^{-1} \le$ E/p $\le$ 800 V $\cdot$ cm$^{-1} \cdot$ Torr^{-1} range.[16,17] We obtained

E/p, V $\cdot$ cm^{-1} $\cdot$ Torr^{-1}:	5	10	15	20
E(0)/p, V $\cdot$ cm^{-1} $\cdot$ Torr^{-1}:	450	615	740	850
d, 10^{-3} cm:	2	1,36	1,1	0,94
φ, V:	450	428	410	400

If the electron density is reduced to 10^{10} cm^{-3}, the value of φ rises to 25 kV and may represent a considerable fraction of the total applied voltage.

2. Excitation of active laser levels

The power supplied to the active medium in a laser can be distributed in various ways between the vibrational, rotational, translational, and electronic degrees of freedom of molecules. The efficiency of the selective excitation of specified degrees of freedom and, therefore, the excitation of the active laser levels, are governed by the electron energy distribution $F(t, \epsilon)$.

The electron energy distribution satisfies the rate equation

$$\frac{\partial F}{\partial t} = -\frac{\partial J_q}{\partial \varepsilon} + \left(\frac{\partial F}{\partial t}\right)_v + \left(\frac{\partial F}{\partial t}\right)_{ex} + \left(\frac{\partial F}{\partial t}\right)_{in}, \tag{10}$$

where

$$J_q = \frac{\alpha}{3}\left(F - 2\varepsilon\frac{\partial F}{\partial \varepsilon}\right) \tag{11}$$

is the flux of electrons in the energy space, governed by the electric field;[18]

$$\alpha = \frac{e^2 E^2}{2m(\omega^2 + v_{eff}^2)} v_{eff}, \tag{12}$$

is the rate of acquisition of energy by an electron from a field of intensity E and frequency ω; e and m are the charge and mass of an electron; v_{eff} is the frequency of elastic collisions of electrons. The other terms on the right-hand side of Eq. (10) correspond to changes in $F(\epsilon, t)$ due to the excitation of vibrational

and electronic levels and due to the ionization.

Elastic collisions, recombination, trapping, and the arrival of electrons from an external ionization source are all ignored in Eq. (12) because we can easily show that they have practically no influence on the electron energy distribution.

The collision term $(\partial F/\partial t)_v$ is

$$\left(\frac{\partial F}{\partial t}\right)_v = \sum_m N_0 \{\sigma_{0m}(\varepsilon + \hbar\omega_{0m})F(\varepsilon + \hbar\omega_{0m})v(\varepsilon + \hbar\omega_{0m}) - \sigma_{0m}(\varepsilon)F(\varepsilon)v(\varepsilon)\}, \quad (13)$$

where N_0 is the concentration of molecules, $\sigma_{0m}(\varepsilon)$ is the excitation cross section of the m-th vibrational level by a quantum of energy $\hbar\omega_{0m}$, and $v(\varepsilon)$ is the velocity of electrons.

It is well known that only the first few (about four) vibrational levels are excited effectively in molecular gases.[19] Since a typical vibrational quantum energy is ~0.1 eV and the vibrational structure of a molecule is excited most effectively in the range ~1—3 eV, Eq. (13) can be rewritten in the form

$$\left(\frac{\partial F}{\partial t}\right)_v = -\frac{\partial J_v}{\partial \varepsilon}, \quad J_v = \alpha^*(\varepsilon)F, \quad (14)$$

where

$$\alpha^*(\varepsilon) = N_0 v(\varepsilon) \sum_m \sigma_{0m}(\varepsilon)\hbar\omega_{0m}$$

represents the rate of loss of energy by electrons in the excitation of the vibrational levels. In practice, the function $\alpha^*(\varepsilon)$ differs from zero only in a narrow (compared with the ionization potential) Δ-like region in the vicinity of the point $\varepsilon = i$, which corresponds to the maximum of $\alpha^*(\varepsilon)$. Consequently, we may assume that

$$\alpha^*(\varepsilon) = \alpha^*(i)\Delta\delta(\varepsilon - i).$$

It follows from Eq. (10) that at the point $\varepsilon = i$ the electron-energy distribution function changes in accordance with the relationship

$$F(t, i+0) = F(t, i-0)\exp\left(-\frac{2}{3}\frac{\alpha^*(i)}{\alpha}\frac{\Delta}{i}\right). \quad (15)$$

Physically the ratio $R = F(t, i+0)/F(t, i-0)$ is the probability of the penetration of an electron beyond the barrier formed by the vibrational levels of a molecule. If $R \ll 1$, practically all the electron energy is transferred to the vibrational levels of a molecule; conversely, if $R \sim 1$ the energy acquired by electrons from the field is lost in the excitation of the electronic levels and in the ionization. In the case of a molecular gas laser, using the rotation-vibrational transitions, the condition $R \ll 1$ is preferable from the energy point of view; conversely, if the laser action is due to transitions between the electronic levels, we must satisfy the condition $R \sim 1$.

EXPERIMENTAL METHOD

The experiments were carried out in enclosures of different volume. The active region was varied from 4 to 13 cm. A beam of fast electrons (~700 keV) was used as the source of ionizing radiation. The beam current was 10—20 A/cm^2 and the duration of the electron pulses was 10^{-8} sec. The electron beam was generated in an electron gun described in[19]. Figure 1 shows a chamber in which the active region was 13 cm long. This chamber consisted of the following parts. A Plexiglas block 7 was fitted with two aluminum electrodes. The lower electrode 1 was solid, whereas the
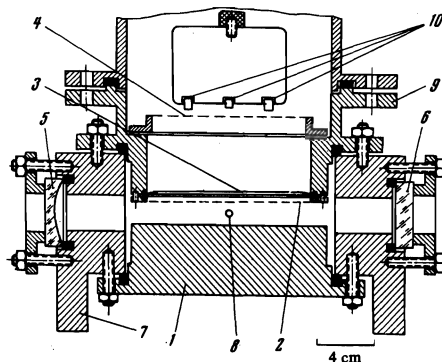

FIG. 1. Chamber of a CO_2 electric ionization laser: 1—lower electron; 2—steel grid; 3—Mylar film; 4—electron-gun anode; 5—opaque mirror; 6—semitransparent mirror; 7—chamber casing; 8—aperture for the admission of gas; 9—upper electrode; 10—electron-gun cathodes.
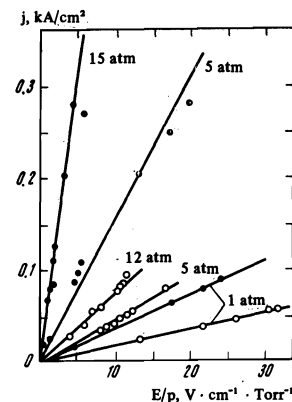

FIG. 2. Dependences of the density of the electric current pulses on the parameter E/p obtained for several typical nitrogen (black dots) and carbon dioxide (open circles) pressures.

upper electrode 9 had an aperture of 130×16 mm, which was closed by a 50-μ thick Mylar film 3. A steel grid 2 was welded 2 mm from the Mylar film. The Mylar film separated the evacuated zone of the electron accelerator from the main chamber filled with the active gas. The upper part of the figure shows a grid-like anode of an electron gun 4 and three cold tungsten cathodes 10. These cathodes were made as described in [20]. The working mixture of gases was admitted into the chamber via an aperture 8. The chamber was fitted with an opaque mirror 5 (radius of curvature 3 m) and a semitransparent mirror 6. The latter mirror was made by depositing a multilayer dielectric interference coating or a gold film on NaCl, Ge, or ZnSe.

The current passing through the gas was measured with a Rogowski loop. The laser radiation energy was measured with a calorimeter and the duration of the laser pulses was determined with the aid of a gold-doped germanium photoresistor. The electrodes were subjected to a voltage provided by a low-inductance capacitor of 10—30 nF capacitance. This capacitor was charged to a voltage of ~50 kV. The gases used in the chamber were of technical purity.

We photographed the emission from the gap between the laser electrodes and the spark which resulted spontaneous breakdown in the compressed gas mixture. These photographs will not be given in the present paper. The brightness of the emission from the gap was many orders of magnitude lower than the brightness of the spontaneous breakdown spark. The emission was visually barely noticeable and the region between the electrodes emitted uniformly.

EXPERIMENTAL RESULTS

Figure 2 shows the dependence of the amplitude of electric current density on the parameter E/p for several typical values of nitrogen and carbon dioxide pressures. The amplitude of the current density was independent of the electrode material and of the polarity of the applied voltage. The lifetime of free electrons and the nature of the decay of the current after the end of the electron beam pulse varied with the composition of the gas filling. In pure nitrogen and in mixtures with small amounts of carbon dioxide the relatively slow electron recombination mechanism predominated and the current decayed hyperbolically with a recombination constant $\sim 2 \times 10^{-7}$ cm^3/sec. In pure carbon dioxide and in mixtures with high concentrations of this gas the important process was the trapping of electrons which reduced the carrier lifetime as well as the current amplitude, and increased the rate of decay of the current. The dependence of the amplitude of the current density on the pressure and electric field could be described by the empirical formula

$$j = Ap^{\alpha}(E/p)^{\delta}. \tag{16}$$

For carbon dioxide the relevant parameters are $\alpha \approx 0.5$ and $\beta \approx 1.1$, whereas for pure nitrogen $\alpha \approx 1$, $\beta \approx 0.9$; the quantity A is a constant. Equation (16) demonstrates that Ohm's law is satisfied and that avalanche multiplication of electrons does not occur in the gas. Moreover, it shows that the rise of the amplitude of the current with increasing electric field is solely due to an increase in the drift velocity of electrons.

The energy evolved in the gas during the passage of an electric current in fields $E > 100$ V/cm exceeded considerably the energy provided by the fast beam electrons. The latter contribution was $\sim 4 \times 10^{-4}$ J $\cdot$ cm^{-3} $\cdot$ atm^{-1}. The specific energy W evolved in nitrogen during the flow of the electric current is plotted in Fig. 3 as a function of the parameter E/p. The dependence given in this figure is in agreement with the empirical formula $W \propto (E/p)^{\gamma}$, where $\gamma \approx 2$. Similar curves were obtained for carbon dioxide and for mixtures of nitrogen, carbon dioxide, and helium. All the mixtures containing carbon dioxide exhibited a fall in

FIG. 5. Pressure dependences of the specific threshold pumping energy for helium-free mixtures. Dielectric mirrors ($T_1 = 5\%$, $T_2 = 0$); $\lambda = 10.6 \mu$.

FIG. 6. Photograph of a gold mirror in the resonator damaged by a laser radiation pulse.

FIG. 7. Dependences of the maximum gain on the pressure (a) and on the composition of CO_2:N_2 mixtures (b). The points represent the experimental values and the continuous curves are the results of calculations.

the energy input. This fall occurred in the range $E/p \approx 9$ V $\cdot$ cm^{-1} $\cdot$ Torr^{-1} and was evidently due to the attainment of an effective electron temperature corresponding to a high value of the trapping cross section.

Figure 4 gives the dependence of the threshold value of the parameter E/p on the pressure in several mixtures. The addition of helium reduced the laser threshold but it also reduced the spark breakdown voltage. Figure 5 gives the dependence of the threshold pumping energy on the pressure in the various mixtures containing only carbon dioxide and nitrogen.

Figure 6 is a photograph of the gold (semi-transparent) mirror damaged by the laser radiation. The burnt-out parts of the mirrors corresponded to the maxima in the distribution of the intensity of the various transverse laser modes over the mirror surface. A single transverse mode could be easily obtained by a suitable tuning of the mirrors.

The gain of the active medium was calculated from the known values of the reflection coefficients of the mirrors and of the distance between the mirrors under threshold conditions. Figure 7 shows the dependences of the maximum values (obtained near the spark breakdown region) of the gain on the pressure and composition of the mixture. It is evident from this figure that the gain reached its maximum in a range of pressures above 1 atm and that this maximum shifted in the direction of higher pressures when the concentration of nitrogen was increased.

Calorimetric measurements of the laser output energy enabled us to determine the laser efficiency. The
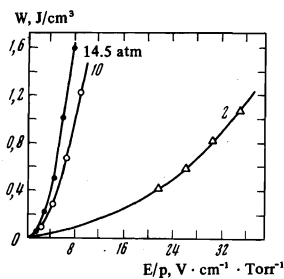
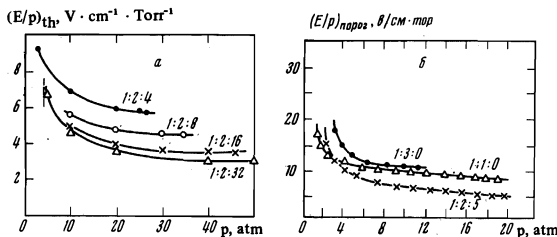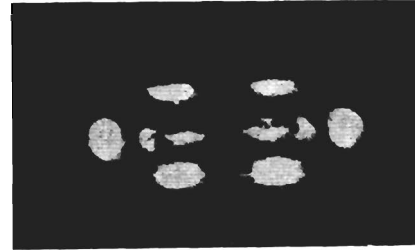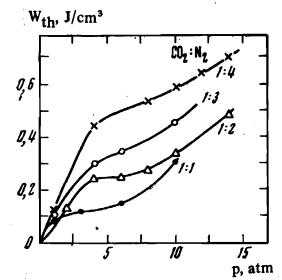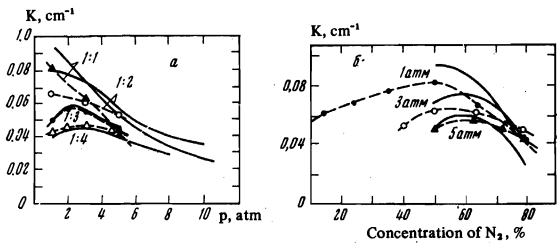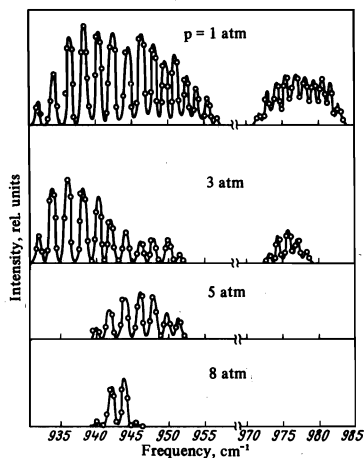FIG. 3. Dependence of the specific input energy on the parameter E/p for nitrogen.

FIG. 4. Pressure dependences of the threshold value of the parameter E/p for CO_2:N_2:He mixtures. The results plotted in Fig. 4a were obtained for dielectric-coated mirrors. The dashed vertical line represents the breakdown threshold.

FIG. 10. Dependence of the maximum specific output power on the pressure in a CO_2 laser.

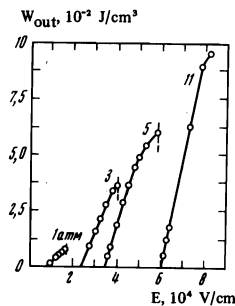FIG. 8. Emission spectra of a CO_2 electric ionization laser obtained at various pressures.

FIG. 9. Dependences of the specific output energy on the electric field plotted for different pressures of the CO_2:N_2 (1:2) working mixture. The breakdown field E_{br} is indicated by vertical dashed lines.

maximum efficiency was 25% for a mixture of carbon dioxide with nitrogen in the ratio 1:2.

The emission spectrum of the laser was recorded by replacing one of the mirrors with a plane diffraction grating covered with 150 lines/mm. The radiation was extracted through the second mirror. A single transverse mode was isolated and the resolution inside the laser resonator was improved by introducing a stop of 3 mm in diameter. The distance between the grating and the second mirror was of the order of 20 cm. Figure 8 shows the emission spectra of the laser obtained at different gas pressures. It is evident from this figure that the laser action occurred in 15 rotational lines of the P branch and in 10 lines of the R branch. Thus, the tunable frequency range was 930—985 cm^{-1}.

The specific output energy of a CO_2 electric ionization laser with an active region 4 cm long is plotted as a function of the electric pumping field in Fig. 9. At low pressures the rise of the specific output energy was limited by the spark breakdown in the gas which occurred when the voltage reached the static breakdown value; at high pressures this energy was limited by the ability of the mirrors to withstand laser radiation (see curve for p = 11 atm).

DISCUSSION OF EXPERIMENTAL RESULTS

Measurements of the current-voltage characteristics and of the energy input demonstrated that the electric current in the gas was governed by the electron mobility (this was true of electron beam currents of ~10—20 A/cm^2 density). The density of the current in the gas and of the energy input were calculated using nominal data on the drift velocity of the electrons. The results of these calculations were in good agreement with the experimental data. The cathode drop of the potential was not measured but the good agreement between theory and experimental results indicated that this drop represented a small fraction of the total voltage applied between the electrodes.

The mechanisms of the excitation and relaxation of the levels in low-pressure (1—50 Torr) carbon dioxide lasers are now well known. The experimental investiga-
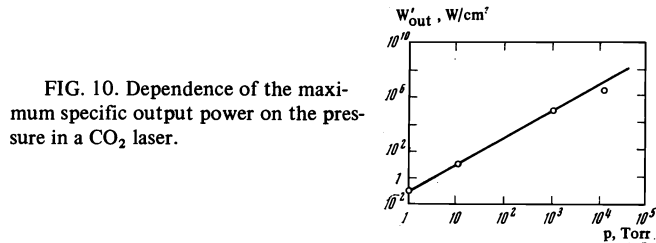
tions of the transversely excited atmospheric (TEA) lasers and the results reported in the present paper indicate that an increase in the pressure of the working mixture to tens of atmospheres does not alter basically the elementary excitation process. The rates of the relaxation processes increase quadratically with the pressure and the width of the levels is directly proportional to the pressure. The rate of excitation of the levels by electron impact and the rate of transfer of this excitation by collisions also increase quadratically with the pressure. Thus, the kinetics of the excitation of the active levels at high pressures (up to tens of atmospheres) is basically similar to the kinetics of excitation at low pressures. Simple calculations show that under quasi-steady-state conditions the excitation of the active medium with sufficiently short pulses generate an output laser power (per unit volume of the active medium) which increases quadratically with the pressure. Figure 10 gives the calculated pressure dependence of the specific output power. The two lower points represent the experimentally obtained data for low-pressure CO_2 gas-discharge lasers. The two upper points represent the results obtained in the present investigation. It is evident from Fig. 10 that an increase in the pressure of the working gas by a factor of 10^3 increases the specific output power by a factor of $~10^6$.

We solved earlier the rate equations describing the excitation and relaxation of the active levels. We assumed that the population of the vibrational levels of the carbon dioxide molecules resulting from direct electron impact was slight compared with the population resulting from collisions with the excited nitrogen molecules. An analysis of the solutions of these rate equations yielded the following expression for the population inversion:

$$\Delta N \approx \frac{W}{(1+\delta)\hbar\omega}\left(1 - \frac{1}{1+\delta}\frac{t^*}{\tau_{CO_2}}\right). \quad (17)$$

Here, W is the specific energy supply to the gas; δ is the ratio of the concentrations of the N_2 and CO_2 molecules; $\hbar\omega$ is the energy quantum corresponding to a transition of the CO_2 molecule from the level v = 0 to the level v = 1; τ_{CO_2} is the relaxation time of the $00°1$ level of the CO_2 molecule; t^* is the time needed to reach maximum inversion.

The value of t^* is given by the following expression:

$$t^* = \frac{1}{2\Omega}\ln\frac{\Lambda+2\Omega}{\Lambda-2\Omega}, \quad (18)$$

$$\Omega = \left[\frac{\Lambda^2}{4} - \frac{\alpha(N_{N_2}+N_{CO_2})}{(1+\delta)\tau_{CO_2}}\right]^{1/2}, \quad \Lambda = \alpha(N_{N_2}+N_{CO_2})+\frac{1}{\tau_{CO_2}},$$

where N_{N_2} and N_{CO_2} are the concentrations of the N_2 and CO_2 molecules; α is the rate constant in the case of inelastic collisions of the CO_2 molecules with the N_2 molecules. According to the published data, $\alpha \approx 5 \times 10^{-13}$ cm^3/sec.[21]

The population inversion and, consequently, the gain of the active medium in a CO_2 electric ionization laser are governed, as in the case of low-pressure CO_2 gas-

N. G. Basov et al.

discharge lasers, by the energy supply to the gas. The experimental results indicate that the specific energy input increases superlinearly with the pressure and the width of the active levels is directly proportional to the pressure. Therefore, the gain of the active medium in an electric ionization laser may reach values much higher than the maximum values of the gain in a gas-discharge CO_2 laser. Moreover, the value of the gain can easily be controlled by varying the degree of ionization of the gas.

The expression for the gain can be written in a form similar to the well-known formula for a gas-discharge CO_2 laser:[15]

$$K(\nu) = \frac{c^2}{8\pi^2\nu^2}\frac{hcB_4}{kT}\sum_{J'}\frac{(2J'+1)\Delta\nu_{J'}A_{12}{}^{J'}\chi(\nu-\nu_{J'})}{(\Delta\nu_{J'})^2+(\nu-\nu_{J'})^2} \quad (19)$$

$$\times\left\{N_4-N_2\frac{B_4}{B_2}\exp\left[\frac{hcB}{kT}F(J')\right]\right\}\exp\left[-\frac{hcB_4}{kT}J'(J'+1)\right].$$

Here N_1 and N_2 are, respectively, the concentrations of the carbon dioxide molecules at the upper and lower laser levels; ν is the frequency of the emitted radiation; B_1 and B_2 are the rotational constants of the upper and lower levels; T is the temperature of the gas mixture; J is the rotational quantum number; $\Delta\nu J'$ is the width of the J'-th level; $F(J') = 2(J'+1)$, if $J' = J'' + 1$ (R branch) and $F(J') = -2J'$ if $J' = J'' - 1$ (P branch). This formula makes allowance for the overlap of the neighboring vibration-rotational lines at high pressures. At these pressures the static spark breakdown field increases with increasing pressure at a rate which is well below the linear law (this is governed by the quality of the surface treatment of the electrodes, the presence of easily ionizable impurities, etc.). Therefore, the rise of the energy supplied to the gas mixture slows down at high pressures.

The continuous curves in Fig. 7 represent the values of the gain calculated using Eqs. (17) and (18) and the experimental values of the energy supplied to the gas. We can see that the calculated curves are in good agreement with the experimental points. The experimental values of the gain obtained at high pressures (the highest pressure at which laser action was observed was ~50 atm) and the good agreement between the calculated and experimental curves demonstrate that no new quenching processes appear at high pressures.

The addition of helium to the working mixture increases the energy acquired by the gas. This results in a corresponding increase in the gain and a reduction in the laser threshold (Fig. 4). The increase in the energy input and the change in the impact broadening coefficient governing the width of the gain profile, which occur on addition of helium, are such that the change in the laser threshold calculated using Eqs. (17) and (18), derived on the assumption of fast relaxation of the lower laser level in the absence of helium, is in agreement with the experimental data. Thus, we may assume that at high pressures the addition of helium basically increases the gain (for a constant value of the pumping electric field) because of an increase in the energy input. However, the maximum value of the gain of the mixtures containing helium is less than the gain of the mixtures free of helium. This experimental observation can be attributed to a considerable reduction in the spark breakdown voltage which results from the addition of helium. Obviously, the optimal mixture for high values of the specific output energy is that containing one part of carbon dioxide for every two parts of nitrogen; this
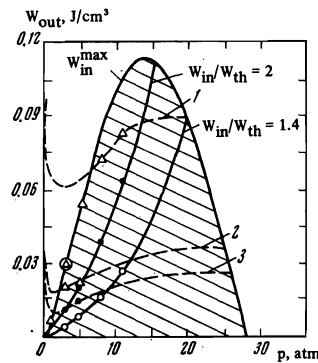

FIG. 11. Pressure dependences of the specific output energy for the $CO_2:N_2$ (1:2) mixture. The continuous curves represent the results of calculations (W_{in} is the input energy) and the points are the experimental data. The dashed lines are the limitations imposed on the output energy by the damage to the resonator mirrors caused by the laser radiation: 1—dielectric mirror on ZnSe; 2—dielectric mirror on Ge; 3—gold mirror on Ge.

mixture should be free of helium and water vapor. The specific output energy obtained for this mixture was $0.033 \text{ J} \cdot \text{cm}^{-3} \cdot \text{atm}^{-1}$ at low pressures (up to 2 atm) and over 0.1 J/cm^3 at high pressures.

Figure 11 shows the calculated pressure dependence of the maximum value of the specific output energy for a mixture containing carbon dioxide and nitrogen in the $1:2$ ratio. The upper curve W_{max} represents the specific output energy limited by the spark characteristics of the gas. The calculated curves are applicable to a laser with an active region 4 cm long. It is evident from Fig. 11 that there is a range of pressures at which the specific energy has its maximum value. In this range, the laser threshold can be exceeded quite strongly. As the pressure is increased, the laser threshold (expressed in terms of the electric field) increases almost linearly with the pressure (Figs. 7 and 9), whereas the static electric breakdown field rises sublinearly with the pressure. Therefore, at some pressure the threshold field intensity becomes equal to the static breakdown field and the laser action can no longer be obtained. This point is reached at ~30 atm (Fig. 11).

If the length of the active region is increased, the laser threshold is reduced and the laser action can be achieved at much higher pressures. The curves lying within the shaded region in Fig. 11, which begins at the origin, represent the pressure dependences of the specific output energy for different degrees of excess over the laser threshold. If the radiation stability of the mirror is insufficiently high, the specific output energy may be limited by the strength of the mirrors. Figure 11 shows several such curves for different mirrors. The pressure dependences of W_{max} obtained for different compositions of the working mixture intersect the pressure axis at different points. For example, in the case of mixtures containing a considerable amount of helium (see, for example, Fig. 4b), the low-pressure dependence of W_{max} intersects the pressure axis near 8 atm and the high-pressure dependence intersects the same axis at a pressure of the order of 120 atm. We were unable to reach pressures of 120 atm for technical reasons (the foil separating the electron accelerator from the working chamber was too weak).

The electric ionization lasers discussed in the present paper have several important advantages over other gas lasers. These ionization lasers combine a very high efficiency, a high specific output energy, and the ability to generate a single mode at high output powers.

The impact broadening of the rotation-vibrational levels of the CO_2 molecule occurs at high pressures

and leads to an overlap of the neighboring rotation-vibrational lines. The frequency dependence of the gain becomes smooth, i.e., free of dips, at pressures in excess of 10−20 atm. Consequently, the width of the gain profile rises rapidly up to 100 cm^{-1} and it becomes possible to tune the frequency smoothly within an interval of 100 cm^{-1} as well as to form pulses of ~10^{-12} sec duration.[5,22] In the present investigation we achieved smooth tuning within 20% of the separation between the rotation-vibrational lines at which laser action took place. Since these tuning experiments were carried out on a short laser (the length of the active region was ~4 cm), we were unable to tune the laser smoothly in a wide frequency interval. Calculations showed that smooth tuning should be possible at working pressures in excess of 8 atm in lasers with an active region over 20 cm long. The use of mixtures containing carbon dioxide of different isotopic compositions should make it possible to halve this pressure. The electric ionization method for the excitation of gases should also be suitable for the excitation of electronic levels of such molecules as H_2, Xe_2, N_2, and so on. In these gases the electric field should be of the order of or higher than the static breakdown value and the duration of the pulses should be less than the typical time needed for the development of an avalanche as a result of the Townsend multiplication of electrons.

[1] C. K. N. Patel, Phys. Rev. Lett. 12, 588 (1964).

[2] R. Dumanchin and J. Rocca-Serra, C. R. Acad. Sci. 269B, 916 (1969).

[3] A. J. Beaulieu, Appl. Phys. Lett. 16, 504 (1970).

[4] O. R. Wood, E. G. Burkhardt, M. A. Pollack, and T. J. Bridges, Appl. Phys. Lett. 18, 112 (1971).

[5] N. G. Basov, E. M. Belenov, V. A. Danilychev, and A. F. Suchkov, Kvantovaya Elektron (Moscow) No. 3, 121 (1971). [Sov. J. Quant. Electron. 1, 306 (1971)].

[6] C. A. Fenstermacher, M. J. Nutter, J. P. Rink, and K. Boyer, Bull. Amer. Phys. Soc. 16, 42 (1971). C. A. Fenstermacher, M. J. Nutter, W. T. Leland, and K. Boyer, Appl. Phys. Lett. 20, 56 (1972).

[7] R. K. Garnsworthy, L. E. S. Mathias, and C. H. H. Carmichael, Appl. Phys. Lett. 19, 506 (1971).

[8] N. G. Basov, V. A. Danilychev, and Yu. M. Popov, Kvantovaya Elektron. (Moscow) No. 1, 29 (1971) [Sov. J. Quant. Electron. 1, 18 (1971)].

[9] V. M. Andriyakhin, E. P. Velikhov, S. A. Golubev, S. S. Krasil'nikov, A. M. Prokhorov, V. D. Pis'mennyĭ, and A. T. Rakhimov, ZhETF Pis. Red. 8, 346 (1968) [JETP Lett. 8, 214 (1968)].

[10] G. G. Dolgov-Savel'ev, V. V. Kuznetsov, Yu. L. Koz'minykh, and A. M. Orishich, Zh. Prikl. Spektrosk. 12, 737 (1970).

[11] A. V. Eletskiĭ and B. M. Smirnov, Dokl. Akad. Nauk SSSR 190, 809 (1970) [Sov. Phys.-Dokl. 15, 109 (1970)].

[12] J. J. Thomson and G. P. Thomson, Conduction of Electricity Through Gases, 3rd ed., 2 vols., Cambridge University Press (1928−1933).

[13] Yu. B. Afanas'ev, E. M. Belenov, O. V. Bogdankevich, V. A. Danilychev, S. G. Darznek, and A. F. Suchkov, Kratk. Soobshch. Fiz. FIAN No. 11, 23 (1970).

[14] B. M. Koval'chuk, V. V. Kremnev, and G. A. Mesyats, Dokl. Akad. Nauk SSSR 191, 76 (1970) [Sov. Phys.-Dokl. 15, 267 (1970)].

[15] N. G. Basov, E. M. Belenov, V. A. Danilychev, O. M. Kerimov, I. B. Kovsh, and A. F. Suchkov, ZhETF Pis. Red. 14, 421 (1971) [JETP Lett. 14, 285 (1971)].

[16] S. C. Brown, Basic Data of Plasma Physics, MIT Press, Cambridge, Mass. 1959 (Russ. Transl., Gosatomizdat, M., 1961).

[17] L. B. Loeb, Fundamental Processes of Electrical Discharges in Gases, Wiley, New York, 1939 (Russ. Transl., Gostekhizdat, M., 1950).

[18] Ya. B. Zel'dovich and Yu. P. Raĭzer, Zh. Eksp. Teor. Fiz. 47, 1150 (1964) [Sov. Phys.-JETP 20, 772 (1965)].

[19] G. J. Schulz, Phys. Rev. 135, A988 (1964).

[20] V. A. Danilychev and D. D. Khodkevich, Prib. Tekh. Eksp. No. 3, 157 (1971).

[21] R. L. Taylor and S. Bitterman, Rev. Mod. Phys. 41, 26 (1969).

[22] N. G. Basov, E. M. Belenov, V. A. Danilychev, and A. F. Suchkov, ZhETF Pis. Red. 14, 545 (1971) [JETP Lett. 14, 375 (1971)].